Giant Nernst Effect due to Fluctuating Cooper Pairs in Superconductors

M. N. Serbyn*, M. A. Skvortsov*, A. A. Varlamov† and V. Galitski**

*Landau Institute for Theoretical Physics, Chernogolovka, Moscow Region, 142432, Russia
Moscow Institute of Physics and Technology, Moscow 141700, Russia
†COHERENTIA-INFM, CNR, Viale del Politecnico 1, I-00133 Rome, Italy
**Joint Quantum Institute and CNAM, Department of Physics, University of Maryland, College Park, MD 20742-4111, USA

Abstract. A theory of the fluctuation-induced Nernst effect is developed for a two-dimensional superconductor in a perpendicular magnetic field. First, we derive a simple phenomenological formula for the Nernst coefficient, which naturally explains the giant Nernst signal due to fluctuating Cooper pairs. The latter signal is shown to be large even far from the transition and may exceed by orders of magnitude the Fermi liquid terms. We also present a complete microscopic calculation of the Nernst coefficient for arbitrary magnetic fields and temperatures, which is based on the standard definition of heat current vertices. It is shown that the magnitude and the behavior of the Nernst signal observed experimentally in disordered superconducting films can be well understood on the basis of superconducting fluctuation theory.

Keywords: Nerst effect, supercondictors
PACS: 74.40.+k, 74.25.Fy, 72.15.Jf

INTRODUCTION

A series of recent experimental studies have revealed an anomalously strong thermomagnetic signal in the normal state of the high-temperature superconductors [1, 2, 3, 4, 5, 6, 8, 7] and disordered superconducting films [9, 10]. In the pioneering experiment [1], Xu *et al.* observed a sizeable Nernst effect in the $La_{2-x}Sr_xCuO_4$ compounds up to 130 K, well above the transition temperature, T_c. This and further similar experiments on the cuprates have sparked theoretical interest in the thermomagnetic phenomena. Theoretical approaches to the anomalously large Nernst-Ettingshausen effect currently include models based on the proximity to a quantum critical point [11], vortex motion in the pseudogap phase [2, 13, 12], as well as a superconducting fluctuation scenario [16, 14, 15]. While the two former theories are specific to the cuprate superconductors, the latter scenario should apply to other more conventional superconducting systems as well. Very recently, a large Nernst coefficient was observed in the normal state of disordered superconducting films [9, 10]. These superconducting films are likely to be well-described by the usual BCS model and, hence, the new experimental measurements provide an indication that the superconducting fluctuations are likely to be the key to understanding the underlying physics of the giant thermomagnetic response.

Various groups have previously calculated the fluctuation-induced Nernst coefficient in the vicinity of the classical transition [18, 17, 16, 14, 15]. However, these analyses were limited to the case of very weak magnetic fields and temperatures close to the zero-field transition, when Landau quantization of the fluctuating Cooper pair motion can be neglected. In experiment, however, other parts of the phase diagram (in particular strong fields) are obviously important and how the quantized motion of fluctuating pairs would figure into the thermomagnetic response has remained unclear. Here we clarify this physics, explaining the origin of the giant fluctuation Nernst-Ettingshausen effect, and develop a complete microscopic theory of Gaussian superconducting fluctuations at arbitrary magnetic fields and temperatures above the mean-field transition line [19].

QUALITATIVE DISCUSSION

We start with a qualitative discussion of the Nernst effect. Consider a conductor in the presence of a magnetic field, H_z, and electric field, E_y, directed along the z- and y-axes respectively. The charged carriers (of charge q) subject to these crossed fields acquire a drift velocity $\bar{v}_x = cE_y/H_z$ in the x-direction. The latter would result in the appearance of a transverse drift current $j_x^{(d)} = nq\bar{v}_x$. When the circuit along x-axis is broken, no current flows, and the drift of carriers is prevented by the spacial variation of the electric potential: $\nabla_x\varphi = -E_x = (nqc/\sigma)(E_y/H_z)$, where σ is the conductivity. Due to electroneutrality, this generates the spacial gradient of the chemical potential: $\nabla_x\mu(n,T) + q\nabla_x\varphi = 0$, which corresponds to the appearance of the transverse temperature gradient $\nabla_x T = \nabla_x\mu(d\mu/dT)^{-1}$ along the x-direction. Hence, the Nernst coefficient can be expressed in terms of the temperature derivative of the chemical potential:

$$\nu_N \equiv \frac{E_y}{(-\nabla_x T)H_z} \sim \frac{\sigma}{nq^2c}\frac{d\mu}{dT}. \qquad (1)$$

To verify Eq. (1), consider, for example, a degenerate electron gas ($q = -|e|$). In this case, the conductivity is given by the Drude formula, $\sigma = ne^2\tau/m$, and the chemical potential $\mu(T) = \mu_0 - (\pi^2T^2/6)(d\ln\nu/d\mu)$, where $\nu(\mu)$ is the density of states. Therefore one easily reproduces the value of the Nernst coefficient in a $3D$ normal metal: $\nu_N = \pi^2T\tau/(6mcE_F)$ [21, 20], where τ is the elastic scattering time (here and below $\hbar = k_B = 1$). Thus the Nernst effect in metals is small due to the large value of the Fermi energy E_F.

We note that the regime of applicability of the qualitative Eq. (1) is expected to coincide with that of the quasiclassical Drude formula. Equation (1) should be relevant to the description of classical Aslamazov-Larkin fluctuations and provide a correct order-of-magnitude estimate of the effect. As shown below, Eq. (1) does in fact remain quantitatively valid in a very wide quasiclassical parameter regime. We note however that one should be careful in applying Eq. (1) to quantitatively describe other systems, especially those where quantum transport dominates.

The simple form of Eq. (1) suggests that in order to get a large Nernst signal, *a strong temperature dependence of the chemical potential of carriers is required.* This simple and intuitive result alone may shed light on the physics behind the strong Nernst signal often seen in various superconductors. Indeed, a strong temperature-dependence of the chemical potential can be achieved in the vicinity of the transition where the fluctuating Cooper pairs appear side by side with the normal electrons. These excitations are unstable, have the characteristic lifetime of order $\tau_{\text{GL}} = \pi/8(T - T_c)$, and form an interacting Bose gas with a variable number of particles. In two dimensions, their concentration is $n^{(2)}_{\text{c.p.}}(T) = (mT_c/\pi)\ln[T_c/(T - T_c)]$ [22].

Near transition, the chemical potential of the fluctuating pairs can be found by identifying its value in the Bose distribution to give $n^{(2)}_{\text{c.p.}}(T)$ above. This leads to $\mu^{(2)}_{\text{c.p.}}(T) = T_c - T$. Since $d\mu^{(2)}_{\text{c.p.}}/dT = -1$, the fluctuation contribution to the Nernst signal exceeds parametrically the Fermi liquid term. In this sense it is similar to the fluctuation diamagnetism (which also exceeds the Landau/Pauli terms and is effectively a correction to the perfect diamagnetism of a superconductor).

Based on the qualitative Eq. (1) and using the known expression for paraconductivity in a magnetic field, $\sigma_{\text{fl}} = (e^2/2\epsilon)F(\epsilon/2\tilde{h})$ [22], one can estimate the value of the Nernst coefficient due to fluctuating Cooper pairs in the Ginzburg-Landau (GL) region:

$$\nu^{(2)}_N(T,H) \sim \frac{1}{mc}\frac{F(x)}{T - T_c} \sim \begin{cases} [mc(T-T_c)]^{-1}, & x \gg 1, \\ (meDH)^{-1}, & x \ll 1, \end{cases} \qquad (2)$$

$$F(x) = x^2\left[\psi(1/2 + x) - \psi(x) - 1/(2x)\right], \qquad (3)$$

where $x = \epsilon/2\tilde{h}$, $\epsilon = \ln(T/T_c)$ and $\tilde{h} = H/\widetilde{H}_{c2}(0)$ are the reduced temperature and magnetic field, $\widetilde{H}_{c2}(0) = 4cT_c/\pi eD$ is the linearly extrapolated value of the upper critical field, and D is the diffusion coefficient. The estimate (2) corresponds to the results in the GL region [16, 18]. We will see below that Eq. (2) indeed provides an order-of-magnitude estimate of the Nernst effect close to the classical transition point, thus giving an additional justification of qualitative arguments leading to Eq. (1).

MICROSCOPIC CALCULATION

General framework

We now proceed with the microscopic calculation of the Nernst coefficient,

$$\nu_N(T,H) = R_\square\beta^{xy}/H, \qquad (4)$$

where $R_\square = 1/\sigma_{xx}$, and $\beta^{\alpha\beta}$ is the thermoelectric tensor relating the transport heat current $\mathbf{j}^Q_{\text{tr}}$ to the applied electric field $\mathbf{E}$ in the absence of a temperature gradient:

$$j^{Q\alpha}_{\text{tr}} = T\beta^{\alpha\beta}E^\beta. \qquad (5)$$

In Eq. (4) we neglect the contribution of the diagonal component, β^{xx}, since it is small in the parameter T/E_F even in the presence of fluctuations [22]. Thus our aim will be to find the fluctuation contribution to the off-diagonal component, β^{xy}.

First we recall a deep relation between thermomagnetic effects and magnetization as emphasized by Obraztsov [23] already in 1965 (later on his arguments have been widely used in Refs. [24, 25, 16]): In the presence of a magnetic field, the measurable transport heat current $\mathbf{j}^Q_{\text{tr}}$ differs from the microscopic heat current $\mathbf{j}^Q$ by the circular magnetization current $\mathbf{j}^Q_M = c\mathbf{M}\times\mathbf{E}$, where $\mathbf{M}$ is the induced magnetization. As a result, the thermoelectric tensor $\beta^{\alpha\beta}$ in Eq. (5) can be found as a sum of the kinetic, $\tilde{\beta}^{\alpha\beta}$, and thermodynamic, $\beta^{\alpha\beta}_M$, contributions:

$$\beta^{\alpha\beta} = \tilde{\beta}^{\alpha\beta} + \beta^{\alpha\beta}_M, \qquad \beta^{\alpha\beta}_M = \epsilon^{\alpha\beta\gamma}cM^\gamma/T. \qquad (6)$$

To calculate the kinetic term, $\tilde{\beta}^{\alpha\beta}$, we employ the Matsubara-Kubo approach and express it via the thermal

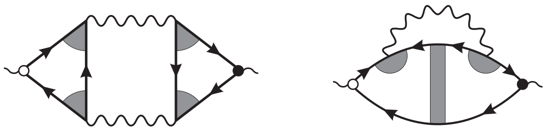

FIGURE 1. The Aslamazov-Larkin (AL) and density-of-states (DOS) diagrams for the thermoelectric response $\tilde{\beta}^{xy}$. The DOS diagram has a symmetric counterpart. The white and black circles correspond to the different heat and electric vertices, the shadowed blocks represent cooperons, and the wavy lines denote the fluctuation propagator (see text). All objects on these graphs are generally matrices in the Landau basis.

and quantum mechanical averaging of the electric-heat currents correlator $Q^{\alpha\beta}(\omega_\nu) = \langle j^{e\alpha}(-\omega_\nu) j^{Q\beta}(\omega_\nu)\rangle$. Then $\tilde{\beta}^{\alpha\beta}$ can be found by analytic continuation from bosonic Matsubara frequencies, $\omega_\nu = 2\pi T\nu$, to real frequencies:

$$\tilde{\beta}^{\alpha\beta} = \frac{1}{T}\lim_{\omega\to 0} \mathrm{Im}\, \frac{Q^{\alpha\beta}(-i\omega+0)}{\omega}. \qquad (7)$$

The thermodynamic term $\beta_M^{\alpha\beta}$ accounts for the magnetization heat current $\mathbf{j}_M^Q$ [23]. It is expressed in terms of the fluctuation magnetization, $M(T,H)$, which has been calculated previously in the GL region [27, 26, 22] and at low temperatures, close to $H_{c2}(0)$ [28].

Our goal now is to evaluate the linear response operator $Q^{xy}(\omega_\nu)$ and analytically continue it to real frequencies. We follow Ref. [28] and perform calculations in the Landau basis, without expanding the Green functions, propagators, current and heat vertices in the magnetic field. This guarantees that gauge invariance is preserved and allows to access the high-field regime. The fluctuation part of the correlator $Q^{xy}(\omega_\nu)$ is generally represented by ten diagrams [28, 22]. However, in the case of the Nernst effect, the Maki-Thompson contribution can be shown to be exactly zero and some of the DOS diagrams turn out to be less singular: The graphs containing three cooperons (see Fig. 1) are dominant. The positive Aslamazov-Larkin (AL) term dominates in the classical Ginzburg-Landau (GL) region and competes with the negative density-of-states (DOS) contribution everywhere else. These AL and DOS contributions, and the fluctuation magnetization are given by [29]

$$Q_{\mathrm{AL}}^{xy}(\omega_\nu) = -4\nu_H T \sum_{\Omega_k}\sum_{n,m} \hat{q}_{mn}^{x} B_{nm}^{(e)} L_n(\Omega_k) \hat{q}_{nm}^{y} B_{nm}^{(Q)} L_m(\Omega_{k+\nu}), \qquad (8)$$

$$2Q_{\mathrm{DOS}}^{xy}(\omega_\nu) = 4\nu_H T \sum_{\Omega_k}\sum_{n,m} \hat{q}_{mn}^{x} \Sigma_{nm}^{(e,Q)} \hat{q}_{nm}^{y} L_n(\Omega_k), \qquad (9)$$

$$M^z = -\frac{\partial}{\partial H}\nu_H T \sum_{\Omega_k}\sum_{n} \ln L_n^{-1}(\Omega_k). \qquad (10)$$

Here $L_n(\Omega_k) = -\nu^{-1}\left[\ln(T/T_c) + \psi_n(|\Omega_k|) - \psi(1/2)\right]^{-1}$ is the fluctuation propagator, $\psi_n(\Omega)$ is a short-hand notation

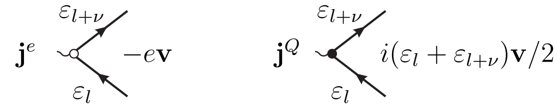

FIGURE 2. Electric-current (left) and heat-current (right) vertices (ε_l and $\varepsilon_{l+\nu}$ are the fermionic Matsubara energies).

for $\psi[1/2 + (\Omega+\alpha_n)/4\pi T]$, with $\alpha_n = (4eDH/c)(n+1/2)$ being the Landau spectrum, $\nu_H = eH/\pi c$, and the matrix elements of the momentum operator in the Landau basis are given by $\hat{q}_{mn}^{x,y} = \sqrt{eH/c}\binom{i}{1}(\sqrt{m}\,\delta_{m,n+1} \mp \sqrt{n}\,\delta_{n,m+1})$.

Electric and heat current blocks

We now calculate exactly the three-Green-function blocks, $B_{nm}^{(e)}(\Omega_k,\omega_\nu)$ and $B_{nm}^{(Q)}(\Omega_k,\omega_\nu)$, with two cooperons and electric or heat vertices shown in Fig. 2. We note here that there exists a long-standing controversy of the proper definition of a heat current and, more generally, the applicability of Kubo-type linear response theory for thermal transport. In our microscopic calculations, we do assume that the latter holds and use the standard definition of the heat current vertex, $i(\varepsilon_l + \varepsilon_{l+\nu})\mathbf{v}/2$ [22], which is known to reproduce all known results, e.g., in a Fermi gas and interacting Fermi liquids. We also evaluate the six-Green-function block with three cooperons and electric and heat vertices, $\Sigma_{nm}^{(e,Q)}(\Omega_k,\omega_\nu)$ and find ($\omega_\nu \geq 0$):

$$B_{nm}^{(e)}(\Omega_k,\omega_\nu) = e\nu D\left[\frac{\psi_m(\omega_\nu + |\Omega_k|) - \psi_n(|\Omega_k|)}{\omega_\nu + \alpha_m - \alpha_n} + \frac{\psi_n(\omega_\nu + |\Omega_{k+\nu}|) - \psi_m(|\Omega_{k+\nu}|)}{\omega_\nu - \alpha_m + \alpha_n}\right], \qquad (11)$$

$$B_{nm}^{(Q)}(\Omega_k,\omega_\nu) = \frac{-i\nu D}{2} \times\left[\frac{(\Omega_k - \alpha_m)\psi_m(|\Omega_k| + \omega_\nu) - (\Omega_{k+\nu} - \alpha_n)\psi_n(|\Omega_k|)}{\omega_\nu + \alpha_m - \alpha_n} + \frac{(\Omega_{k+\nu} + \alpha_n)\psi_n(|\Omega_{k+\nu}| + \omega_\nu) - (\Omega_k + \alpha_m)\psi_m(|\Omega_{k+\nu}|)}{\omega_\nu + \alpha_n - \alpha_m}\right], \qquad (12)$$

$$\Sigma_{nm}^{(e,Q)}(\Omega_k,\omega_\nu) = -ie\nu D^2\left[\frac{\Omega_{k+\nu} - \alpha_n}{\omega_\nu + \alpha_m - \alpha_n}\psi_n'(|\Omega_k|) - \frac{\Omega_{k+\nu} + \alpha_n}{\omega_\nu - \alpha_m + \alpha_n}\psi_n'(|\Omega_{k+\nu}| + \omega_\nu) - \frac{\Omega_k - \alpha_m}{(\omega_\nu + \alpha_m - \alpha_n)^2}\left(\psi_m(|\Omega_k| + \omega_\nu) - \psi_n(|\Omega_k|)\right) + \frac{\Omega_k + \alpha_m}{(\omega_\nu - \alpha_m + \alpha_n)^2}\left(\psi_n(|\Omega_{k+\nu}| + \omega_\nu) - \psi_m(|\Omega_{k+\nu}|)\right)\right]. \qquad (13)$$

Results in various asymptotic regions

The general calculation of Eqs. (8)–(10) is straightforward but cumbersome. However, one can identify nine qualitatively different regions of the phase diagram (Fig. 3), where the asymptotic behavior has a simple analytical form. Before proceeding to the corresponding details, we emphasize that the result for the Nernst coefficient is universal in the sense that the function $\beta^{xy}(T,H)$ depends only on T/T_c and $H/H_{c2}(0)$, but not the elastic scattering time τ (unlike conductivity). This universality is due to the magnetization contribution, β^{xy}_M, which regularizes the otherwise divergent (and thus τ-dependent) terms in $\tilde{\beta}^{xy}$. These seemingly accidental cancellations between the two physically distinct terms appear in a wide parameter range and are unlikely to be a coincidence (e.g., they may not occur if a different definition of heat vertices is used). Therefore, these remarkable cancellations provide a strong evidence that the standard definition of the heat vertices is indeed appropriate to describe the effect.

Ginzburg-Landau region

We start by discussing *the classical regime close to the critical temperature* T_c: The regions I, II, III in Fig. 3 are characterized by $\epsilon = \ln(T/T_c) \ll 1$ and $\tilde{h} = H/\widetilde{H}_{c2}(0) \ll 1$. In these domains, only the classical AL contribution is important and is given by [cf. Eq. (2)]: $\tilde{\beta}^{xy} = 2\beta_0 F(x)/x$, where $x = \epsilon/2\tilde{h}$, $\beta_0 = k_B e/\pi\hbar = 6.68$ nA/K is the quantum of thermoelectric conductance, and the function $F(x)$ is given by Eq. (3). The magnetization contribution to the observable β^{xy} [see Eq. (6)] is given by

$$\beta^{xy}_{\mathrm{M}} = \beta_0 \Big[\ln \frac{\Gamma(1/2+x)}{\sqrt{2\pi}} - x\psi(1/2+x) + x \Big]. \qquad (14)$$

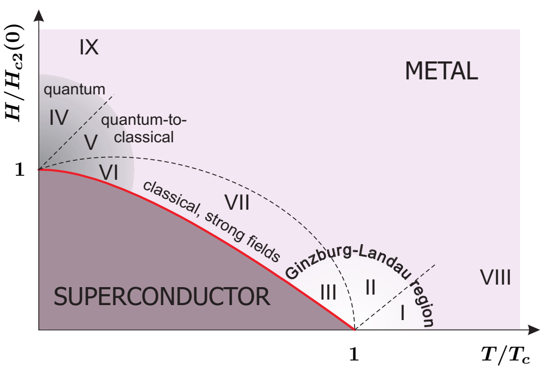

FIGURE 3. Different asymptotic regions for the fluctuation Nernst effect on the (H,T) phase diagram. Landau quantization of the Cooper pair motion is important in the regions II–VII and IX.

In the limit of vanishingly small magnetic fields $\tilde{h} \ll \epsilon$ (region I), we find $\tilde{\beta}^{xy} = \beta_0(\tilde{h}/2\epsilon)$, which is two times larger than the result of Refs. [16, 14, 22] where the same microscopic Matsubara-Kubo approach has been used. The additional factor is due to the complicated analytic structure of the heat-current block (12) overlooked in the previous diagrammatic calculations [16, 14, 22], but properly accounted for in Ref. [17]. Note that our diagrammatic calculation also differs from by a factor-of-two from the result of the phenomenological Ginzburg-Landau approach [22]. This difference may be related to a more fundamental issue (as compared to a calculational mistake) and may signal, e.g. a problem with the definition of the heat currents within time-dependent Ginzburg-Landau (TDGL) theory or/and diagrammatics. The exact origin of the factor-of-two discrepancy remains unclear at this stage.

Thus in the region I, the magnetization contribution $\beta^{xy}_{\mathrm{M}} = -\beta_0(\tilde{h}/6\epsilon)$ cancels only 1/3 of $\tilde{\beta}^{xy}$, and the final result appears to be four times larger than that of Refs. [16, 14, 22]:

$$\beta^{xy}_{\mathrm{I}} = \beta_0 \frac{\tilde{h}}{3\epsilon} = \beta_0 \frac{\pi e D H}{12c(T-T_c)}, \qquad \tilde{h} \ll \epsilon \ll 1. \qquad (15)$$

In the limit $\epsilon \ll \tilde{h}$ (region II), and close to the transition line, at $\tilde{h} + \epsilon \ll \tilde{h}$ (region III), we find

$$\beta^{xy}_{\mathrm{II}} = \beta_0 \left[1 - (\ln 2)/2\right], \qquad \epsilon \ll \tilde{h} \ll 1; \qquad (16)$$

$$\beta^{xy}_{\mathrm{III}} = \beta_0 \frac{\tilde{h}}{\epsilon + \tilde{h}} = \beta_0 \frac{H_{c2}(T)}{H - H_{c2}(T)}, \qquad \epsilon + \tilde{h} \ll \tilde{h} \ll 1. \qquad (17)$$

Low-temperature region

Now we turn to the *low-temperature regime close to the upper critical field* $H_{c2}(0) = \pi c T_c/2\gamma e D$ (regions IV, V, VI in Fig. 3), where $\gamma = 1.78\ldots$ is the exponential of the Euler constant. Here role of magnetization term becomes crucial: The $1/T$ divergence of $\beta^{xy}_{\mathrm{M}} = M^z/T$ exactly cancels the divergent contribution originating from $\tilde{\beta}^{xy}$, which is necessary to satisfy the third law of thermodynamics. As a result, the total coefficient β^{xy}_{IV} remains finite in the limit or zero temperature. The exact analytical expression at $t = T/T_c \ll 1$ and $\eta = (H - H_{c2}(t))/H_{c2}(t) \ll 1$ is quite lengthy. We present below only the asymptotic expressions in the regions IV, V, VI.

In the purely quantum limit of vanishing temperature and away from $H_{c2}(0)$ ($t \ll \eta$, region IV), β_{xy} is negative:

$$\beta^{xy}_{\mathrm{IV}} = -\frac{2\beta_0 \gamma t}{9\eta} = -\frac{\beta_0 \pi c T}{9eD[H - H_{c2}(0)]}, \qquad t \ll \eta \ll 1. \qquad (18)$$

This change of sign in thermoelectric response is similar to negative magnetoresistance in the quantum fluctuation transport for the usual electrical conductivity found in Ref. [28] in the vicinity of $H_{c2}(0)$. The sign change is due to the DOS contribution being numerically larger than the positive AL term. In the quantum-to-classical crossover region, where H tends to $H_{c2}(t)$ but remains limited as $t^2/\ln(1/t) \ll \eta \ll t$ (region V), the coefficient β_{xy} is positive:

$$\beta^{xy}_{\mathrm{V}} = \beta_0 \ln(t/\eta), \qquad t^2/\ln(1/t) \ll \eta \ll t \ll 1. \quad (19)$$

Near $H_{c2}(t)$ ($\eta \ll t^2/\ln(1/t)$, region VI), we find:

$$\beta^{xy}_{\mathrm{VI}} = 8\beta_0\gamma^2 t^2/3\eta, \qquad \eta \ll t^2/\ln(1/t) \ll 1. \quad (20)$$

Above the transition line

We also address the full classical region *just above the transition line*, which covers a wide range of temperatures and magnetic fields ($\eta \ll 1$, region VII). In this region, $\tilde{\beta}^{xy}$ is generally comparable to $\beta^{xy}_{\mathrm{M}} = -\beta_0/\eta$, and we obtain

$$\beta^{xy}_{\mathrm{VII}} = \frac{\beta_0}{\eta}\left[1 + \frac{h}{4\gamma t}\frac{\psi''(1/2 + h/4\gamma t)}{\psi'(1/2 + h/4\gamma t)}\right], \qquad \eta \to 0, \quad (21)$$

with $h = H/H_{c2}(0)$. Close to T_c, Eq. (21) matches Eq. (17), while in the limit $T \to 0$ it matches Eq. (20) provided that $\eta \ll t^2/\ln(1/t)$. We note that in deriving Eq. (21), the Landau quantization of the Cooper pair motion was crucial.

Far from the transition line

Finally, we address the "non-singular" *regions VIII and IX far from the transition line*. In this limit, the Kubo contribution $\tilde{\beta}^{xy}$ diverges as $[\ln\ln(1/T_c\tau) - \ln\ln\max(h,t)]$, with $1/\tau$ playing the role of the ultraviolet cutoff of the cooperon modes. Remarkably, the same divergence of the opposite sign occurs in the magnetization contribution β^{xy}_{M}. Hence, the total expression for β^{xy} remains finite:

$$\beta^{xy}_{\mathrm{VIII}} = \beta_0 \frac{eDH}{6\pi cT\ln(T/T_c)}, \qquad (1,h) \ll t; \quad (22)$$

$$\beta^{xy}_{\mathrm{IX}} = \beta_0 \frac{\pi cT}{12eDH\ln[H/H_{c2}(0)]}, \qquad (1,t) \ll h. \quad (23)$$

We see that even far from the transition the fluctuation Nernst coefficient can be comparable or parametrically larger than the Fermi liquid terms. In fact, it is conceivable that in some materials the Cooper channel contribution to thermal transport at low temperatures can be dominant even in the absence of any superconducting transition at all (e.g., if superconductivity is "hidden" by another order).

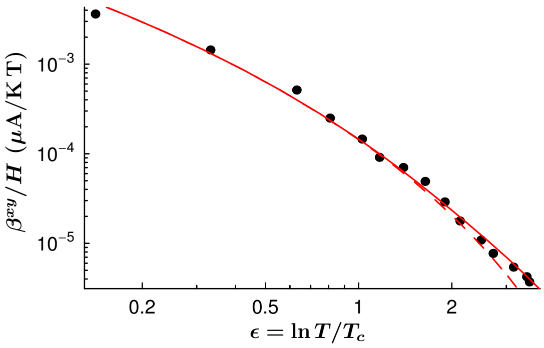

FIGURE 4. Comparison with experiment. Circles: experimental data for $\lim_{H\to 0}\beta^{xy}/H$ vs. $\epsilon = \ln T/T_c$ obtained for the 12.5-nm-thick $Nb_{0.15}Si_{0.85}$ film [9]. Dashed line: theoretical prediction for the strictly 2D geometry. Solid line: theoretical prediction for the real sample [9] with the 2D-3D crossover taken into account.

Comparison with experiment

Plotted in Fig. 4 is a comparison between our theory and the experimentally measured Nernst coefficient [9] for a $Nb_{0.15}Si_{0.85}$ film of thickness $d = 12.5$ nm. The dashed line corresponds to the coefficient $\lim_{H\to 0}\beta^{xy}/H$ in a wide range of temperatures up to $30\,T_c$. We used the diffusion coefficient $D = 0.087$ cm^2/s which is 60% of that reported in Ref. [9] (with $k_F l \sim 1$, the precise determination of D is questionable). Note that far from the transition point ($\epsilon > 2$), the superconducting coherence length $\xi(T)$ becomes shorter than d and 3D nature of diffusion manifests itself. It can be described by substituting $\alpha_n \to \alpha_n + D(\pi p/d)^2$ and performing an additional summation over $p = 0, 1, \ldots$ in Eqs. (8)–(10). The resulting curve is shown in Fig. 4 by the solid line.

CONCLUSION

In summary, we have developed a complete microscopic theory of the fluctuation Nernst effect in a two-dimensional superconductor. Our results provide a natural explanation for a large Nernst signal observed in superconducting films [9, 10] and probably should be relevant to the cuprates. Another interesting theoretical predictions is a slow decay of the transverse thermoelectric response away from the transition line, which is expected to persist well into the metallic phase.

Finally, we remark on a recent alternative approach [30] to precisely the same problem, where the Keldysh nonequilibrium technique has been used. Technical details of the calculation [30] are not available but their findings look pretty similar to our results: They identify exactly the same asymptotic regions on the (H,T) diagram, with the asymptotic expressions coinciding with our Eqs. (15)–(23) up to some numerical factors of order one. In full analogy with our treatment, in Ref. [30] the magnetization term β_M^{xy} was also crucial to regularize the otherwise divergent term $\tilde{\beta}^{xy}$ in the regions IV, VII, IX. Contrary to our approach, Ref. [30] reproduces the TDGL result in the AL region I, thus making a critical reexamination of various approaches to the heat transport highly demanding.

ACKNOWLEDGMENTS

We are grateful to Herve Aubin, Mikhail Feigel'man and Alexei Kavokin for useful discussions. M.N.S acknowledges partial support from Dynasty Foundation and hospitality of the University Paris-Sud. V.G. acknowledges BU visitors program's hospitality. The work of M.N.S. and M.A.S. was partially supported by RFBR Grant No. 07-02-00310.

REFERENCES

1. Z. A. Xu et al., *Nature* **406**, 486 (2000).
2. Y. Wang et al., *Phys. Rev. B* **64**, 224519 (2001).
3. Y. Wang et al., *Phys. Rev. Lett.* **88**, 257003 (2002).
4. C. Capan et al., *Phys. Rev. Lett.* **88**, 056601 (2002).
5. H. H. Wen et al., *Europhys. Lett.* **63**, 583 (2003).
6. Z. A. Xu et al., *Phys. Rev. B* **72**, 144527 (2005).
7. P. Li and R. L. Greene, *Phys. Rev. B* **P76**, 174512 (2007).
8. Y. Wang, L. Li and N. P. Ong, *Phys. Rev. B* **73**, 024510 (2006).
9. A. Pourret et al., *Nature Phys.* **2**, 683 (2006).
10. A. Pourret et al., *Phys. Rev. B* **76**, 214504 (2007).
11. S. A. Hartnoll et al., *Phys. Rev. B* **76**, 144502 (2007).
12. S. Raghu et al., arXiv:0801.2925v2 (2008).
13. D. Podolsky, S. Raghu and A. Vishwanath, *Phys. Rev. Lett.* **99**, 117004 (2007).
14. I. Ussishkin, *Phys. Rev. B* **68**, 024517 (2003).
15. I. Ussishkin and S. L. Sondhi, *Int. J. Mod. Phys. B* **18**, 3315 (2004).
16. I. Ussishkin, S. L. Sondhi and D. A. Huse, *Phys. Rev. Lett.* **89**, 287001 (2002).
17. M. Yu. Reizer and A. V. Sergeev, *Phys. Rev. B* **50**, 9344 (1994).
18. S. Ullah and A. T. Dorsey, *Phys. Rev. Lett.* **65**, 2066 (1990); *Phys. Rev. B* **44**, 262 (1991).
19. M. N. Serbyn, M. A. Skvortsov, A. A. Varlamov and V. Galitski, e-print arXiv:0806.4427.
20. We assume the white-noise disorder, i.e., $\tau(\epsilon)\nu(\epsilon) = \text{const}$.
21. E. H. Sondheimer, *Proc. R. Soc. A* **193**, 484 (1948).
22. A. I. Larkin and A. A. Varlamov, in "The Physics of Superconductors", Eds. K. Bennemann and J. Ketterson, Springer, 2002.
23. Y. N. Obraztsov, *Fiz. Tverd. Tela.* **7**, 573 (1965) [*Sov. Phys. Solid State* **7**, 455-461 (1965)].
24. L. Li et al., *Europhys. Lett.* **72**, 451 (2005).
25. N. R. Cooper, B. I. Halperin, and I. M. Ruzin, *Phys. Rev. B* **55**, 2344 (1997).
26. R. A. Klemm, M. R. Beasley and A. Luther, *Phys. Rev. B* **8**, 5072 (1973).
27. J. Kurkijärvi, V. Ambegaokar and G. Eilenberger, *Phys. Rev. B* **5**, 868 (1972).
28. V. M. Galitski and A. I. Larkin, *Phys. Rev. B.* **63**, 174506 (2001).
29. The unusual subscript order in Eq. (8) is related to the vertex symmetry property: $B_{mn}^{(e)}(\Omega_k, \omega_\nu) = B_{nm}^{(e)}(\Omega_k + \omega_\nu, -\omega_\nu)$.
30. K. Michaeli and A. M. Finkel'stein, e-print arXiv:0812.4268.